Nuclear Magnetic Resonance Solution Structure of an Undecanucleotide Duplex with a Complementary Thymidine Base opposite a 10*R* Adduct Derived from Trans Addition of a Deoxyadenosine N^6-Amino Group to (−)-(7*R*,8*S*,9*R*,10*S*)-7,8-Dihydroxy-9,10-epoxy-7,8,9,10-tetrahydrobenzo[*a*]pyrene[†]

Eric J. Schurter,[‡] Jane M. Sayer,[§] Toshinari Oh-hara,[§] Herman J. C. Yeh,[§] Haruhiko Yagi,[§] Bruce A. Luxon,[||] Donald M. Jerina,[§] and David G. Gorenstein*,[||]

Department of Chemistry, Purdue University, West Lafayette, Indiana 47907, Laboratory of Bioorganic Chemistry, National Institute of Diabetes and Digestive and Kidney Diseases, National Institutes of Health, Bethesda, Maryland 20892, and Department of Human Biological Chemistry and Genetics, University of Texas Medical Branch, NMR Center, Galveston, Texas 77555

Received October 17, 1994; Revised Manuscript Received March 28, 1995[⊗]

ABSTRACT: The solution structure of a modified undecamer duplex containing (−)-(7*R*,8*S*,9*R*,10*S*)-7,8-dihydroxy-9,10-epoxy-7,8,9,10-tetrahydrobenzo[*a*]pyrene covalently bonded through trans ring opening at C10 of the epoxide by the N^6-amino group of deoxyadenosine (dA) was studied. This diol epoxide 1 diastereomer has the benzylic 7-hydroxyl group and the epoxide oxygen cis. The modified nucleotide residue has *R* chirality at C10 of the hydrocarbon (10*R* adduct). The undecamer duplex d($C_1G_2G_3T_4C_5A^*_6C_7G_8A_9G_{10}G_{11}$)·d($C_{12}C_{13}T_{14}C_{15}G_{16}T_{17}G_{18}A_{19}C_{20}C_{21}G_{22}$) has a complementary T opposite the modified dA (dA*6 is the modified dA). Exchangeable and nonexchangeable proton assignments were made using 2D TOCSY, NOESY, and water/NOESY NMR spectroscopy. The hybrid complete relaxation matrix program MORASS was used to generate NOESY distance constraints for iterative refinement using distance-restrained molecular dynamics calculations. The refined structure showed the hydrocarbon intercalated from the major groove between dA*6-T17 and dC5-dG18 base pairs. The modified dA*6 was in the normal anti configuration and showed Watson−Crick base pairing to T17 opposite. The chemical shifts of the hydrocarbon protons and the unusual shifts of sugar protons were accounted for by the intercalated orientation of the hydrocarbon.

Polycyclic aromatic hydrocarbons (PAH) are common environmental contaminants whose metabolism in mammals results in the formation of activated species that are cytotoxic, mutagenic, and/or carcinogenic [reviewed in Thakker et al. (1985, 1988)]. Numerous studies over the past 20 years have indicated that benzo ring diol epoxides in which the epoxide group is located in a bay region of the molecule (Jerina et al., 1976; Jerina & Daly, 1976) are ultimate carcinogens formed upon oxidative metabolism of these hydrocarbons. A prototypical PAH, benzo[*a*]pyrene (BaP), is metabolized by cytochrome P-450 and epoxide hydrolase in liver microsomes from 3-methylcholanthrene-treated rats to give an enantiomeric pair of 7,8-dihydrodiols, of which the (−)-(7*R*,8*R*)-7,8-dihydroxy-7,8-dihydrobenzo[*a*]pyrene is the predominant (≥98%) isomer. Further metabolism of this enantiomer yields a diasteromeric pair of 7,8-diol-9,10-epoxides as a result of oxidation from both faces of the hydrocarbon ring system. The major isomer, (+)-(7*R*,8*S*,9*S*,-10*R*)-7,8-dihydroxy-9,10-epoxy-7,8,9,10-tetrahydrobenzo[*a*]-pyrene [(*R*,*S*,*S*,*R*)-DE2], has the benzylic 7-hydroxyl group and epoxide oxide trans, and the minor isomer, (−)-(7*R*,8*S*,9*R*,10*S*)-7,8-dihydroxy-9,10-epoxy-7,8,9,10-tetrahydrobenzo[*a*]pyrene [(*R*,*S*,*R*,*S*)-DE1], has these group cis (Thakker et al., 1977). Trivial names for these two diasteromers include anti or DE2 and syn or DE1 for the isomers with trans and cis relative stereochemistry, respectively, between the 7-hydroxyl group and epoxide oxides.

For a number of diol epoxides derived from different hydrocarbons, the (*R*,*S*,*S*,*R*)-DE2 isomer is the predominant diol epoxide formed metabolically as well as the most tumorigenic (Jerina et al., 1980, 1984). In contrast, the DE1 isomers are generally not tumorigenic or only weakly so. For diol epoxides (such as those derived from BaP) that lack unusual stereochemical features, the observed low tumorigenic activity for DE1 isomers has been suggested to result from the conformation of the tetrahydro benzo ring, whose two hydroxyl groups prefer a pseudoaxial orientation, in contrast to the pseudoequatorial orientation normally preferred by these groups in DE2 (Chang et al., 1987). A presumptive mechanism for the initiation of cell transformation by diol epoxides involves covalent modification of DNA by nucleophilic attack of DNA bases to open the oxirane ring. If the preferred orientation of the hydroxyl groups influences the conformation of the covalent adducts formed, such conformational differences may be relevant to the enzymatic repair and/or replication of the damaged DNA. Thus it is of considerable interest to compare DNA adducts derived from the DE2 and DE1 diastereomers.

[†] This work was supported by the NIH−NCI Training in Drug and Carcinogen−DNA Interactions (Grant CA09634), NIH Grant AI27744 and NSF Grants BBS8614177 and DIR-9000360.

[‡] Purdue University.

[§] NIH.

[||] University of Texas Medical Branch.

[⊗] Abstract published in *Advance ACS Abstracts,* June 1, 1995.

0006-2960/95/0434-9009$09.00/0

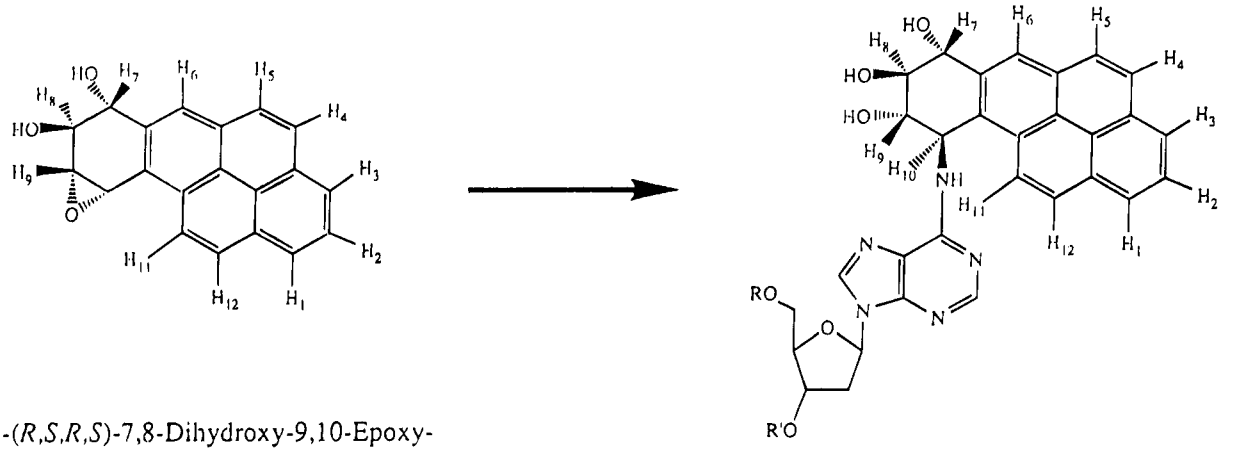

(-)-(*R,S,R,S*)-7,8-Dihydroxy-9,10-Epoxy-7,8,9,10-tetrahydrobenzo[a]pyrene [(-)-(*R,S,R,S*)-DE1]

(*R,S,S,R*)-N^6-[10-(7,8,9-trihydroxy-7,8,9,10-tetrahydrobenzo[a]pyrenyl)]-2'-dexyadenosine [trans DE1(10*R*)-dA Adduct]

FIGURE 1: Trans addition of the exocyclic N^6-amino group of dA to (−)-(7*R*,8*S*,9*R*,10*S*)-7,8-dihydroxy-9,10-epoxy-7,8,9,10-tetrahydrobenzo-[*a*]pyrene [(−)-(*R,S,R,S*)-BaP DE1]. Since the adducts arise by trans attack at C10, configuration of this carbon in the diol epoxide inverts upon adduct formation. A corresponding change in configurational designation also occurs at C9, in this case due to application of the priority rules rather than a change in configuration.

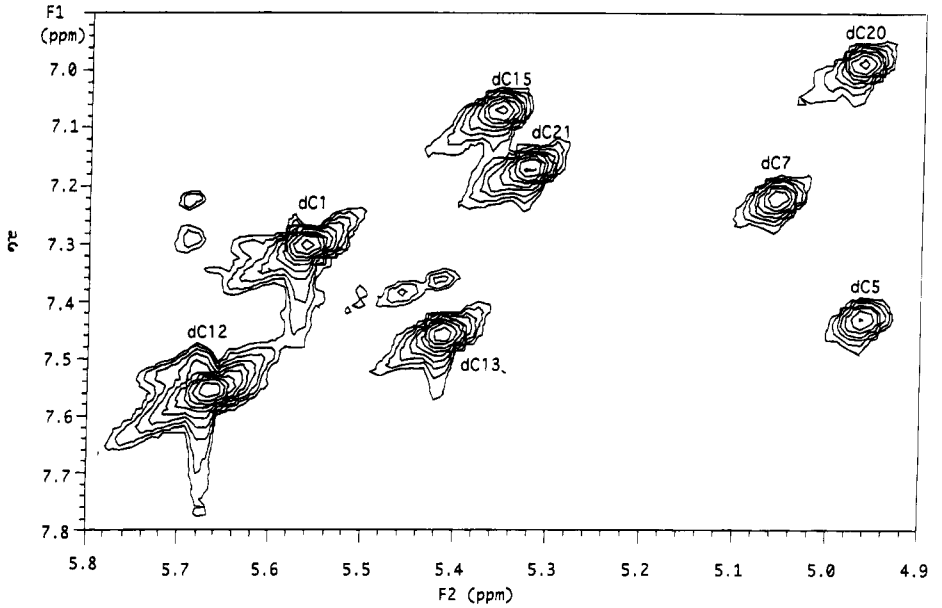

FIGURE 2: TOCSY spectrum (50 ms mixing time) of the dC H5 to H6 region showing all of the cytosine bases. Very small unassigned cross peaks may be attributed to minor conformers or impurities.

Predominant adducts formed upon reaction of diol epoxides with DNA involve ring opening of the epoxide by cis or trans attack of the exocyclic N^2- and N^6-amino groups of guanine and adenine, respectively [reviewed in Jerina et al. (1991) and references therein]. The tumorigenic (*R,S,S,R*)-DE2 isomer reacts preferentially with dG residues in DNA, and such adducts account for the preponderance of mutations in the *HPRT* locus in Chinese hamster V79 cells induced by high doses of this diol epoxide. However, much lower doses such as those from environmental exposure result in a large relative increase in mutations at deoxyadenosine (dA) (Wei et al., 1991, 1993). Thus the biological activity of dA adducts derived from DE1 and DE2 may be substantial.

We have recently described the solution structure of a nonanucleotide duplex containing a benzo[*a*]pyrene−dA adduct corresponding to the trans opening of the epoxide of (−)-(*S,R,R,S*)-DE2 by the N^6-amino group of dA (Schurter et al., 1995). In the present study, we report the structure of an undecanucleotide duplex containing a dA residue modified by trans addition to (−)-(7*R*,8*S*,9*R*,10*S*)-7,8-dihydroxy-9,10-epoxy-7,8,9,10-tetrahydrobenzo[*a*]pyrene in the same sequence context. This oligonucleotide duplex is $d(C_1G_2G_3T_4C_5A^*{}_6C_7G_8A_9G_{10}G_{11})\cdot d(C_{12}C_{13}T_{14}C_{15}G_{16}T_{17}G_{18}A_{19}C_{20}C_{21}G_{22})$ in which the modified dA*6 residue is (7*R*,8*S*,9*S*,10*R*)-N^6-[10-(7,8,9-trihydroxy-7,8,9,10-tetrahydrobenzo[*a*]pyrenyl)]-2′-deoxyadenosine [trans (−)-DE1-(10*R*)-dA adduct] (Figure 1). This represents the first NMR structure of a DNA adduct derived from a DE1 (syn) diastereomer. In both structures reported by us to date, the absolute configuration at the N-substituted benzylic C10 position is *R*. In the present structure, the base opposite the modified dA is the normal Watson−Crick complement, T, whereas our previously reported DE2 adduct duplex had a dG opposite the adducted dA. Data from these and other

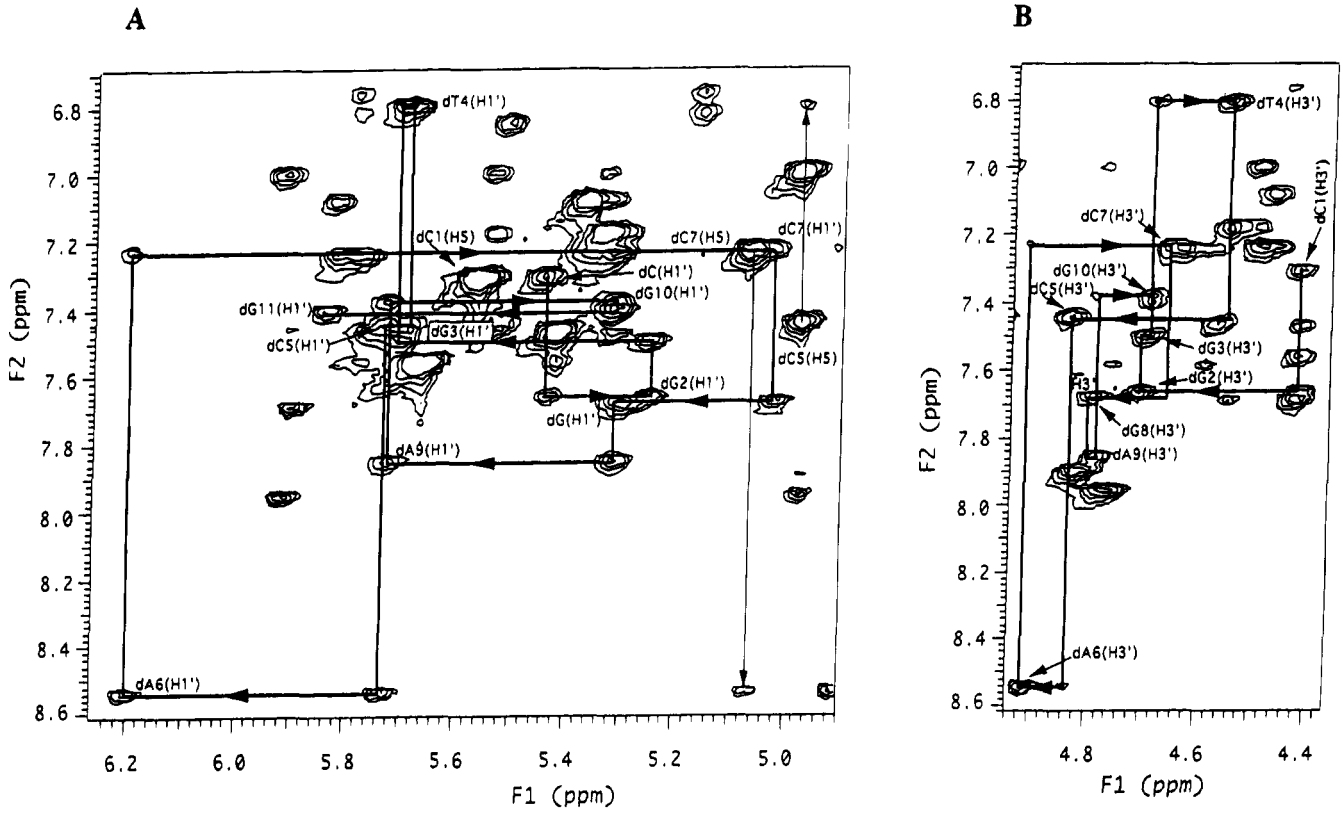

FIGURE 3: Expanded NOESY spectrum (150 ms mixing time) showing the connectivities between the base protons (8.6−6.8 ppm) and (A) sugar H1′ (6.3−5.0 ppm) or (B) H3′ (4.9−4.4 ppm) protons. The connectivities depicted are for the modified strand. The dC H5 to base connectivities are indicated with thin vertical arrows.

Table 1: Chemical Shift Assignments[a] for Sugar Protons of the Undecanucleotide Duplex Containing a Trans (−)-DE1(10*R*)−dA Adduct[b]

		H1′	H2″	H2′	H3′	H4′	H6 or H8	H5	H2	H5′,H5″	Me
						Modified Strand					
5′-	Cyt 1	5.43	2.08	1.57	4.41	3.79	7.30	5.56		3.68, 3.42	
	Gua 2	5.24	2.44		4.71	4.04	7.65			3.85, 3.78	
	Gua 3	5.70	2.42	2.26	4.69	4.15	7.49			3.94, 3.90	
	Thy 4	5.67	1.90	1.51	4.55	3.86	6.79			3.52	0.89
	Cyt 5	5.73	2.30	2.41	4.82	4.05	7.43	4.97			
	Ade 6[c]	6.20	2.70	2.53	4.91	4.30	8.53		7.70	3.89, 3.92	
	Cyt 7	5.02	2.07	1.95	4.62	3.94	7.22	5.06		3.66, 3.88	
	Gua 8	5.31	2.55	2.46	4.79	4.11	7.67			3.82, 3.78	
	Ade 9	5.72	2.59	2.36	4.79		7.84		7.48		
	Gua 10	5.31	2.38	2.22	4.70	4.07	7.37			3.66	
3′-	Gua 11	5.83	2.14	2.07	4.33	3.93	7.40			3.82	
						Complementary Strand					
5′-	Cyt 12	5.69	2.29	2.03	4.41	3.86	7.55	5.66		3.94, 3.52	
	Cyt 13	5.76	2.26	1.97	4.58		7.46	5.42		3.96, 3.85	
	Thy 14	5.81	2.26	1.98	4.63		7.23			3.96, 3.77	1.38
	Cyt 15	5.30	1.49	1.88	4.46	3.79	7.08	5.36			
	Gua 16	5.30	2.21	1.81	4.49	3.92	7.23				
	Thy 17	5.15	1.86	1.55	4.44	3.67	5.78			3.82	−0.20
	Gua 18	4.76	2.47	2.42	4.60		7.57				
	Ade 19	5.91	2.58	2.47	4.77	4.21	7.95		7.45	3.92, 3.88	
	Cyt 20	5.53	1.66	2.07	4.49	3.89	6.99	4.97		3.82, 3.78	
	Cyt 21	5.28	2.04	1.71	4.56		7.17	5.34		3.81, 3.76	
3′-	Gua 22	5.89	2.36	2.10	4.42		7.68			3.92, 3.78	

[a] Chemical shifts are given in parts per million, referenced to HDO (4.65 ppm at 15 °C). [b] Missing chemical shifts could not be unambiguously assigned. The H5′, H5″ protons could not be distinguished and are listed in random order. [c] Ade 6: trans (−)-DE1(10*R*)−dA adduct.

studies make it possible to dissect some of the effects of absolute configuration on the solution structures of BaP-modified oligonucleotides.

EXPERIMENTAL PROCEDURES

Sample Preparation. A previously published synthetic approach for the incorporation of diol epoxide-modified dA phosphoramidites into oligonucleotides was used (Lakshman et al., 1992) to synthesize the undecamer d(CGGTCA*-CGAGG), where dA* represents the modifed dA residue. Purity (≥98%) of the modified oligonucleotide was confirmed by capillary zone electrophoresis in 20 mM phosphate buffer, pH 7.4. Enzymatic degradation to the nucleoside level (Sayer et al., 1991) followed by HPLC [Beckman

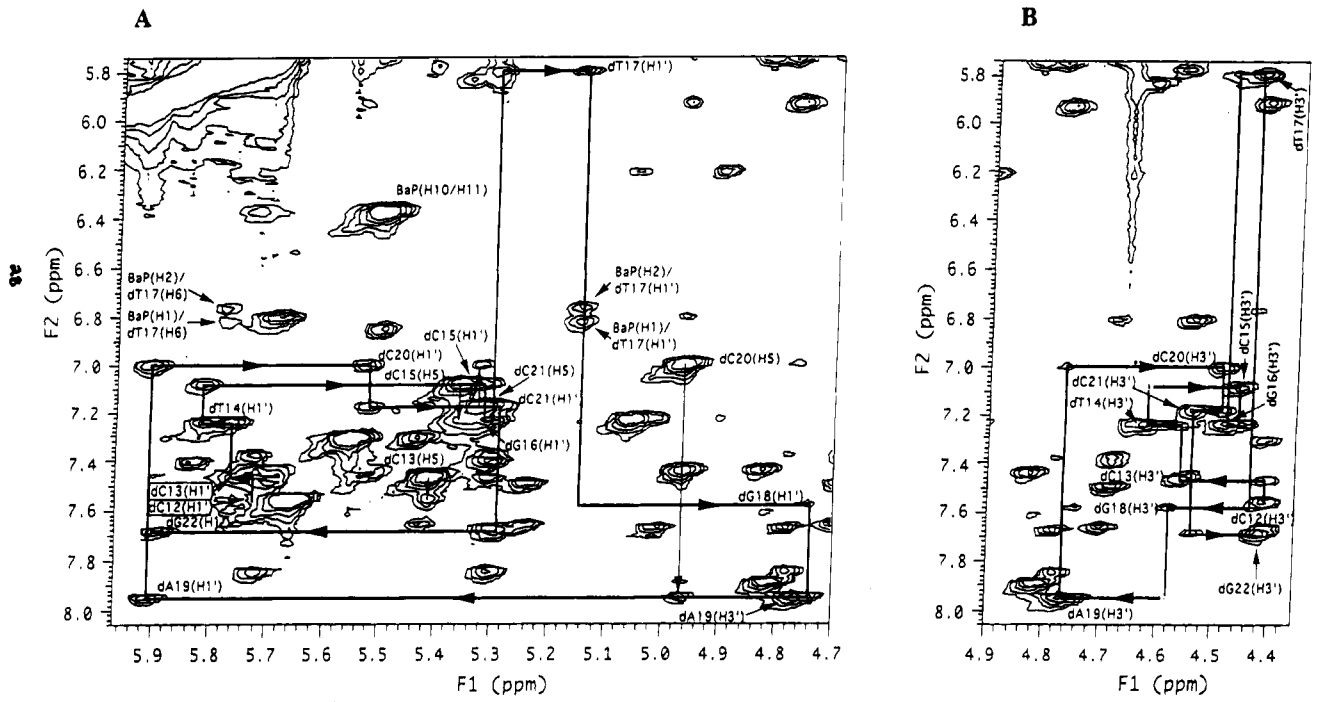

FIGURE 4: Expanded NOESY spectrum (150 ms mixing time) showing the connectivities between the base protons (8.0−5.8 ppm) and (A) sugar H1′ (5.9−4.7 ppm) protons or (B) H3′ (4.8−4.4 ppm) protons. Connectivities depicted are for the complementary strand. The T17 H1′ (5.15 ppm) to dG18 H8 (7.57 ppm) cross peak is not observable. Also, note the very unusual upfield chemical shifts of T17 H6 (5.78 ppm) and dG18 H1′ (4.76 ppm), which are attributable to the intercalated hydrocarbon. Cross peaks between the tetrahydro BaP H1 and H2 protons and T17 H6 and H1′ protons are shown.

Table 2: Chemical Shift Assignments[a] for Hydrocarbon Protons of the Trans DE1(10*R*)−dA Adduct

hydrocarbon protons[b]	chemical shift assignments	hydrocarbon protons[b]	chemical shift assignments
H1	6.81	H7	4.83
H2	6.76	H8	4.02
H3	7.24	H9	3.49
H4	7.55	H10	5.51
H5	7.60	H11	6.36
H6	7.89	H12	6.84

[a] Chemical shifts are given in parts per million referenced to HDO (4.65 ppm at 15 °C). [b] Hydrocarbon protons H1, H2, H3, H4, H5, H6, H11, and H12 are aromatic and H7, H8, H9, and H10 are aliphatic.

Table 3: Chemical Shift Assignments[a] of Labile and Nonlabile Protons in the Watson−Crick Base Pairs for the Undecamer Duplex Containing a Trans (−)-DE1(10*R*)−dA Adduct[b]

base pair	dG H1 or dT H3	dC $4NH_2$[c]	dG $2NH_2$	dC H5
dG2-dC21	12.86	8.32, 6.68		5.34
dG3-dC20	12.44	7.72, 6.16	6.68	4.97
dT4-dA19	13.12			
dC5-dG18	10.76	6.48, 5.72	6.80	4.97
dA*6-dT17[d]	11.48			
dC7-dG16	12.56	7.98, 6.50	6.72	5.06
dG8-dC15	12.66	8.23, 6.73		5.36
dA9-dT14	13.60			
dG10-dC13	12.72	8.14, 6.78		5.42

[a] Chemical shifts are given in parts per million referenced to HDO (4.65 ppm at 15 °C). [b] Missing chemical shifts could not be unambiguously assigned. [c] The first value is the chemical shift of the hydrogen-bonded amino proton. [d] dA*6 = trans (−)-DE1(10*R*)−dA adduct.

Ultrasphere C_{18} column, 4.6 × 250 mm, eluted at 1.2 mL/min with solvent A (50 mM sodium phosphate, pH 7.0, containing 5% MeOH) for 8 min, followed by two successive linear gradients of solvent B (10% H_2O in MeOH) that increased the proportion of B to 10% in 7 min and then to 100% in the next 15 min] gave a ratio of unmodified nucleosides A:T:G:C of 0.9:1.0:5.2:3.0 (theoretical 1:1:5:3). The modified strand was titrated with the complementary strand, d(CCTCGTGACCG), and the end point (1:1 ratio) was determined spectroscopically as described (Schurter et al., 1995). Melting temperatures of duplexes were measured as described (Lakshman et al., 1992). The sample used for the NMR studies contained approximately 310 A_{260} units of duplex and was dissolved in 600 mL of D_2O (99.995%) buffer (100 mM total ionic strength) containing 12 mM Na_2HPO_4, 8 mM NaH_2PO_4, 56 mM NaCl, and 2 mM sodium azide at pH 7.1.

NMR Experiments. A Varian VXR600 (600 MHz) spectrometer at a regulated temperature of 15 °C was used to record the 2D water/NOESY spectra (Ottings et al., 1991). The sample was prepared in 90% H_2O/10% D_2O buffer and the spectrum was recorded at a mixing time of 150 ms. A Varian VXR500 (500 MHz) spectrometer at a regulated temperature of 15 °C was used to record the 2D TOCSY and NOESY spectra in D_2O buffer. The TOCSY spectrum (Bax & Davis, 1985) was recorded at 50 ms mixing time. The NOESY spectra were recorded at 150 and 200 ms mixing times. All spectra were acquired with 4096 points in the t_2 dimension and 1024 t_1 points and then apodized with a shifted sine bell before Fourier transformation. NOESY volumes were taken from the 150 ms mixing time spectra for structural refinement. The NOESY cross-peak intensities between H8 or H6 of the bases and H1′ of the sugar on the same nucleotide residue were used to distinguish qualitatively between syn (strong NOE) and anti (weak NOE) glycosidic torsional angles (Wüthrich, 1986).

NOESY Distance-Restrained Molecular Mechanics/Dynamics Calculations of the Adduct. The Chem3D 3.0 (Cambridge Scientific Computing, Inc.) program was used to generate bond distances, bond angles, and dihedral angles for the modified oligonucleotide duplex. The force field

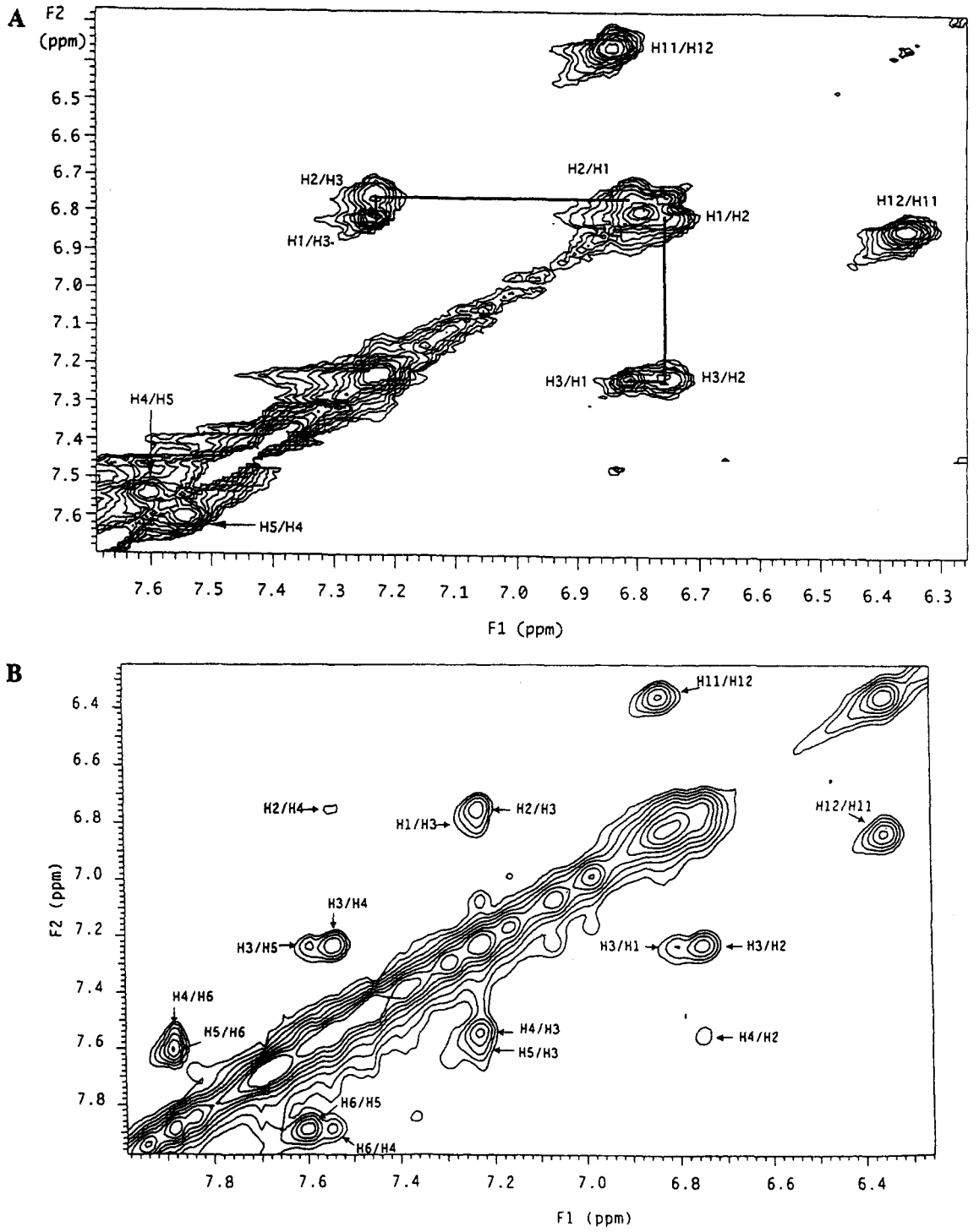

FIGURE 5: (A) TOCSY spectrum (50 ms mixing time) of the aromatic pyrene proton region (H1, H2, H3, H4, H5, H6, H11, H12). The two spin systems H11/H12 and H4/H5 show as single cross peaks. The three-spin system (H1, H2, H3) is indicated with a solid line. (B) NOESY spectrum (150 ms mixing time) of aromatic pyrene proton region.

parameters were adopted from equivalent AMBER4.0 atom types (Weiner & Kollman, 1981), and the partial molecular charges were from ab initio calculations (Hingerty & Broyde, 1985). The AMBER4.0 molecular dynamics program was then used on a Silicon Graphics Indigo XS24 R4000 workstation to generate the starting structure of the adduct in both the duplex B-DNA and A-DNA forms. The MIDAS Plus molecular modeling program (Langridge & Ferrin, 1984) was used to manipulate manually the starting model structures and display the refined structures.

The method of choice for accurately interpreting NOE volumes of interproton distances is the complete relaxation methodology (Keepers & James, 1984). A primary weakness of the complete relaxation matrix method is the need to measure nearly complete NOESY data sets. Fortunately this can be resolved by utilizing the hybrid matrix method. Originally proposed by Kaptein and co-workers (Boelens et al., 1988), the hybrid matrix approach addresses the problem of incomplete experimental data. The solution is to combine the information from the experimental NOESY volumes and calculated volumes, derived from an initial structure. The hybrid volume matrix contains the well-resolved and measureable cross peaks from the NOESY spectrum, while overlapping or weak cross peaks and diagonals are from the

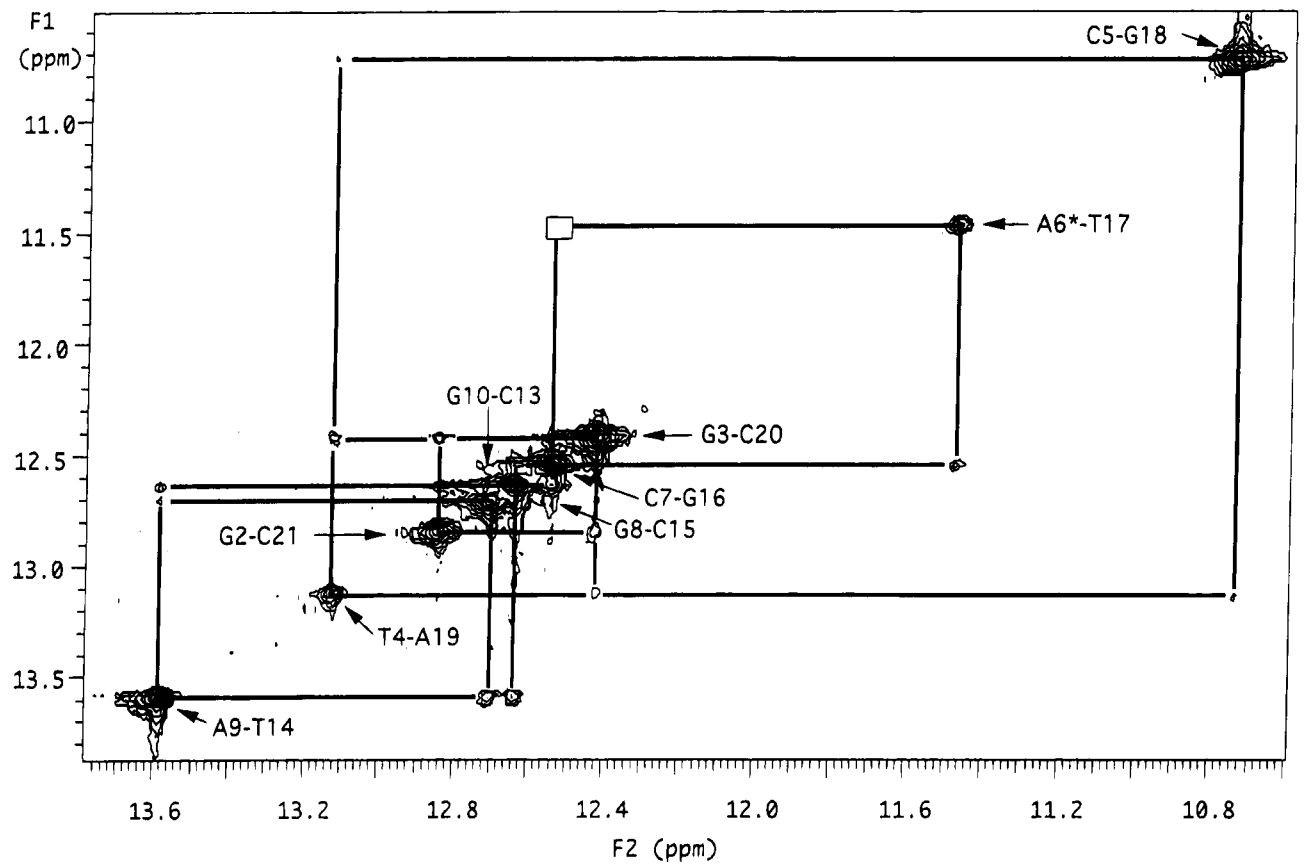

FIGURE 6: H_2O NOESY spectrum (150 ms mixing time) of the 11-mer duplex imino region (C, T, G, and A are dC, T, dG, and dA, respectively). Base-pair-to-base-pair connectivity can be traced from G2-C21 to C5-G18 then from A*6-T17 to G10-C13. The break between C5-G18 and A*6-T17 corresponds to the intercalation site of the hydrocarbon.

Table 4: MORASS/Molecular Dynamics Iterative Refinement Cycles for the Final Structure[a]

iteration	flatwell[b]	% error[c]	H bond[d]	dA6 H2′, H2″ to dC7 H6[e]	BaP H10 to dC5 H2′, H2″[f]	RMS[g]	% E[h]	% T[i]	*R*-factor[j]	$Q(1/6)^k$	total energy[l]	constraint energy[m]
model						3.52	403	210	1.354	0.1378	−469	
1	2	20	6	8	10	0.99	124	115	0.507	0.0939	−882	41
2	3	18	7	8	16	0.76	104	80	0.504	0.0856	−885	43
3	4	16	8	10	16	0.56	82	69	0.499	0.0821	−884	55
4	5	14	8	12	16	0.31	89	56	0.499	0.0758	−887	59
5	6	12	8	14	16	0.15	81	56	0.490	0.0734	−892	94
6	7	10	8	16	16	0.14	70	54	0.474	0.0706	−889	86
7	12	10	8	16	16	0.15	69	49	0.496	0.0700	−892	95

	Energy Decompositions								
iteration	bond	angle	dihed	VDW	elec	H-bond	1-4NB	1-4 ele	E_{pot}
1	9.4	86.0	231.9	−360.2	824.4	−6.0	129.2	−1800.1	−885
3	9.7	89.0	232.9	−361.3	823.8	−5.2	129.7	−1802.3	−884
4	10.0	91.0	232.1	−365.0	822.6	−5.2	129.3	−1801.8	−887
5	9.4	85.6	228.8	−362.8	827.7	−5.6	129.3	−1804.5	−892
6	9.5	88.6	233.6	−357.6	816.2	−5.9	129.2	−1801.6	−888
7	9.6	87.0	233.1	−359.8	817.1	−5.3	129.4	−1803.2	−892

[a] The refinement was started with model-built B-DNA coordinates. [b] Harmonic potential force constant (kilocalories per mole per square angstrom) applied to the flatwell constraints. [c] Half the percent variation in the constraint distance allowed without energy penalty. [d] Hydrogen bonding constraint energy between base pairs. [e] Harmonic potential force constant (kilocalories per mole per square angstrom) applied to the flatwell constraint energy for dA*6 (H2′) to dC7 (H6) and dA*6 (H2″) to dC7 (H6). [f] Harmonic potential force constant (kilocalories per mole per square angstrom) applied to the flatwell constraint energy for dC5 (H2′) to hydrocarbon (H10) and dC5 (H2″) to hydrocarbon (H10). [g] Root mean square error in volumes calculated by MORASS. [h] Percent RMS error in volumes (experimental − theoretical/experimental) calculated by MORASS. [i] Percent RMS error in volumes (experimental − theoretical/theoretical) calculated by MORASS. [j] The *R*-factor is calculated with the following equation where v_{ij}^a = the experimental volume measurement and v_{ij}^b = the calculated volume: *R*-factor = $\{\sum[v_{ij}^a - v_{ij}^b]\}/\sum[v_{ij}^b]$. [k] RMS difference in the $^1/_6$ power of the volumes (Bonvin, 1993). [l] Total energy of structure not including NOESY distance constraint term (kilocalories per mole). [m] Total energy of NOESY distance constraints (kilocalories per mole). [n] Bond, angle, dihed, VDW, elec, H-bond, 1-4NB, and 1-4 ele represent the bond, angle, dihedral angle, van der Waals, electrostatic, hydrogen-bond, 1-4 nonbonded, and 1-4 electrostatic decomposition energies in the AMBER force field, respectively.

calculated spectrum. This hybrid matrix is then used to back-calculate the rate matrix from which the distances are calculated. These new distances are then utilized as input to a restrained molecular dynamics refinement (via simulated annealing) of the structure. Energy minimization of the structure derived from molecular dynamics completes one cycle of refinement. This process is repeated until there is satisfactory agreement between the calculated and observed

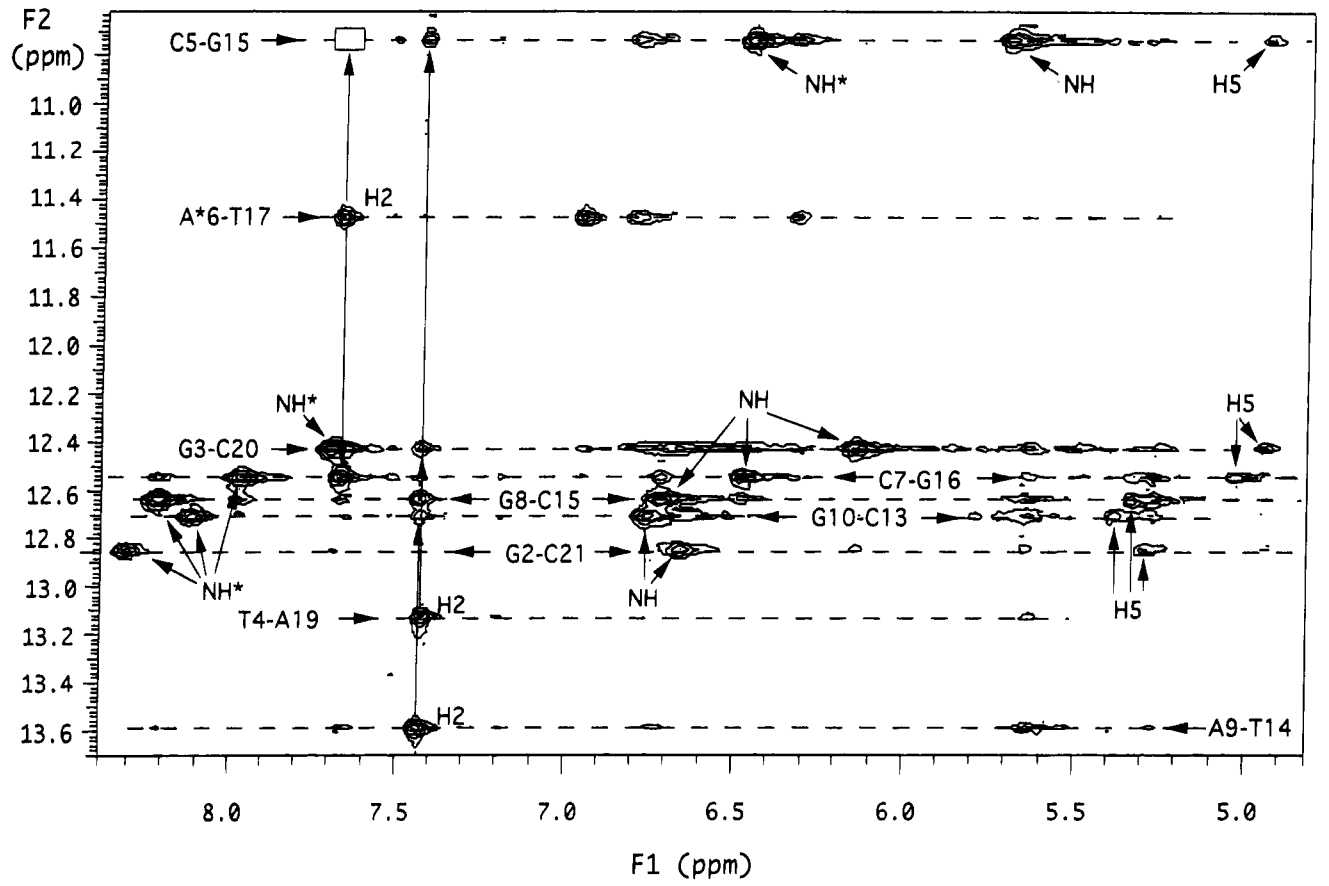

FIGURE 7: H_2O NOESY spectrum (150 ms mixing time) of the undecamer duplex amino region (C, T, G, and A are dC, T, dG, and dA, respectively). The dashed lines indicate the imino proton chemical shift for each base pair. Interbase pair NOEs for the dA H2 protons are indicated with solid arrows. The missing dA*(H2) to C5-G15 NOE corresponds to the intercalation site of the hydrocarbon. NH* = the hydrogen-bonded dC $4NH_2$.

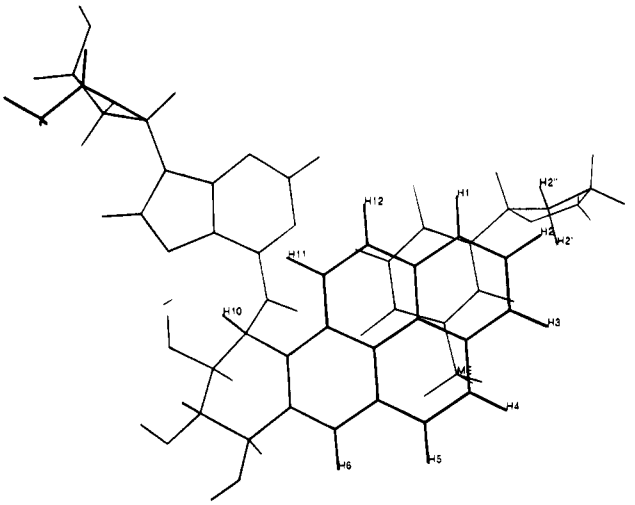

FIGURE 8: Refined structure of the undecanucleotide duplex with a trans (−)-DE1(10*R*)−dA adduct in DNA (viewed along the helical axis, in the 3′ direction of the modified strand). The refined structure shows T17 Me (−0.20 ppm) and H6 (5.78 ppm) protons stacked under the hydrocarbon (BaP) rings, resulting in large upfield chemical shifts. There are NOEs from hydrocarbon protons H1, H2, and H3 to T17 sugar protons; hydrocarbon protons H4, H5, and H6 to T17 Me; hydrocarbon H12 to dA*6 H2; hydrocarbon H10 and H9 to dC5 sugar and base protons.

cross-peak volumes. The hybrid relaxation matrix program MORASS2.0 (Gorenstein et al., 1993) was used to generate a total of 366 NOESY flatwell distance constraints for iterative refinement using distance-restrained molecular dynamics (MD) calculations with a locally modified version of AMBER4.0.

All energy minimization and restrained molecular dynamics calculations were done *in vacuo* with a distance-dependent dielectric to simulate bulk solvation by water. The temperature was started at 100 K and raised to 400 K over 1 ps. Then the temperature was reduced to 300 K over 2 ps and maintained for the remaining 3 ps of the MD run. The coordinates for the last 3 ps of the MD run were averaged, followed by 300 cycles of minimization. The 6-ps block of this simulated annealing (MD and energy minimization) completed one cycle of refinement. This process was repeated until a satisfactory agreement between the calculated and observed cross-peak volumes was obtained. Details are provided in Nikonowicz et al. (1989, 1990).

Convergence was monitored by using equations 1 and 2:

$$\%\ \mathrm{RMS}_{\mathrm{vol}} = \{[(1/N)\sum[(v_{ij}^{a} - v_{ij}^{b})/v_{ij}^{a}]^2]\}^{1/2} \times 100 \quad (1)$$

% $\mathrm{RMS}_{\mathrm{vol}}$ = % T when v_{ij}^{a} = the calculated volume and v_{ij}^{b} = the experimental volume, and % $\mathrm{RMS}_{\mathrm{vol}}$ = % E when v_{ij}^{a} = the experimental volume and v_{ij}^{b} = the calculated volume.

$$Q(^1/_6) = \{[(1/N)\sum[(v_{ij}^{a\ 1/6} - v_{ij}^{b\ 1/6})/v_{ij}^{a\ 1/6}]^2]\}^{1/2} \quad (2)$$

$Q(^1/_6)$ = percent root mean square difference in the $^1/_6$ power of the volumes (Bonvin et al., 1993) when v_{ij}^{a} = the calculated volume and v_{ij}^{b} = the experiment volume.

Convergence was achieved when the % $\mathrm{RMS}_{\mathrm{vol}}$ and $Q^1/_6$ were within the reliability of the experimental volume measurement. Since most structurally important distances

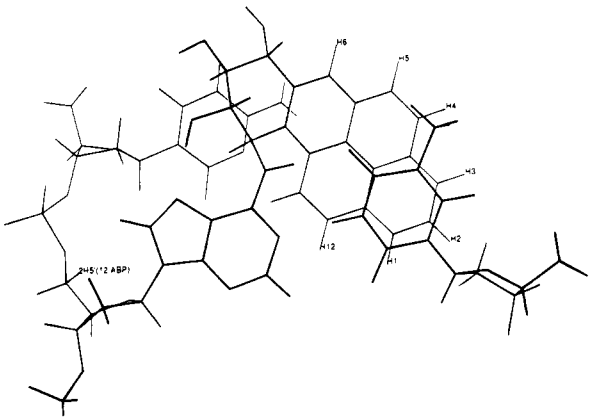

FIGURE 9: Refined structure of the undecanucleotide duplex with a trans (−)-DE1(10*R*)−dA adduct DNA (viewed along the helical axis, in the 5′ direction of the modified strand). The refined structure shows the base of dC5 (modified strand) stacking over the aliphatic portion of the hydrocarbon ring.

were those from longer-range NOEs, and since these small off-diagonal volumes (<2% of the diagonal volumes) are the most sensitive to experimental noise, we feel an acceptable RMS error is 50−60%. This is because a 60% error in the average volume represents an approximate 10% error in the average distances due to the r^{-6} distance dependence to the NOE volume. The *R*-factor is also monitored and is slightly smaller (50%) because the short fixed distances make a major contribution to this value. As shown by our laboratory (Nikonowicz et al., 1989, 1990; Gorenstein et al., 1990) and others (Boelens et al., 1988, 1989; James et al., 1991), 3−5 iterations appear to be adequate to achieve convergence to a "refined" structure.

RESULTS

Nonexchangeable DNA Proton Spectra. TOCSY spectra were used to identify through-bond connectivities in the sugar spin systems and to identify the cytosine base protons (Figure 2 shows the dC H5 to H6 cross peaks). Through-space NOE cross peaks from the NOESY spectra were used to establish the base-to-base connectivities. Figure 3 shows the connectivities for the modified strand in the H1′, H3′ to base proton region. The connectivities were completely traced through the H1′ to base and H3′ to base regions. The dA*6 H8 proton (dA*6 is the modified adenosine) shows a downfield chemical shift. The sequential connectivities in the complementary strand (Figure 4) for the same region show some breaks. The break between T17 H1′ and dG18 H8 corresponds to the site of intercalation of the hydrocarbon. The large upfield chemical shift of T17 H6 was due to stacking directly under the pyrene ring system (the 5′ end of the modified strand is at the top). Furthermore, the upfield shift of the dG18 H1′ proton was also due to stacking with the pyrene rings at the site of intercalation. The H1′, H3′, H6, and H8 assignments were confirmed using several spectral regions. Complete assignments for the base and sugar H1′, H2′, H2″, H3′ protons are given in Table 1.

Nonexchangeable Hydrocarbon Protons. The labeling convention for the hydrocarbon and absolute configuration for the adduct are shown in Figure 1. The coupled proton spin systems of the hydrocarbon were identified using through-bond connectivities in the TOCSY spectra and

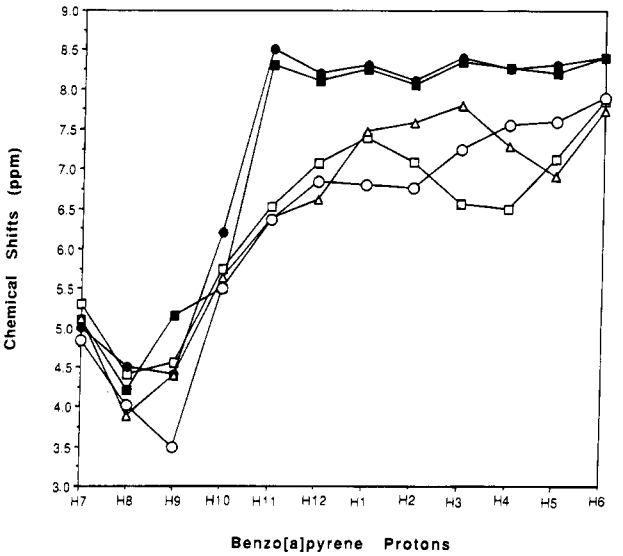

FIGURE 10: Nonexchangeable protons of the hydrocarbon plotted against chemical shift. Plot compares intercalated trans (−)-DE1-(10*R*)−dA adduct of the tetrahydrobenzo[*a*]pyrene moiety (○) of this study, intercalated trans (+)-DE2(10*S*)−dA adduct (△) (Yeh et al., submitted for publication) and intercalated trans (−)-DE2-(10*R*)−dA adduct (□) (Schurter et al., 1995). The trans (+)-DE2-(10*S*)−dG adduct (●) and trans (−)-DE2(*R*)−dG adduct (■) have the hydrocarbon in the minor groove (Cosman et al., 1992; De los Santos et al., 1992).

through-space NOE cross peaks from the NOESY spectra were then used to connect the spin systems. This made it possible to walk completely around the hydrocarbon ring system. Table 2 contains the complete assignment of all protons of the hydrocarbon, and Figure 5 shows the TOCSY and NOESY spectra of the aromatic hydrocarbon protons.

Exchangeable DNA Proton Spectra. All of the exchangeable base protons could be assigned except for the terminal base pairs at each end of the duplex. Table 3 contains the exchangeable proton assignments. The spectra clearly establish the Watson−Crick base pairing between the modified dA*6 and the T17 opposite on the unmodified strand (Figures 6 and 7). The base-to-base connectivity in the imino water/NOESY spectrum shows a break between base pair dC5-dG18 and dA*6-T17 which is presumably due to intercalation of the hydrocarbon between them (Figure 6). Further, the large upfield chemical shift of the dC5-dG18 and dA*6-T17 imino protons is associated with their stacking directly above and below the pyrene ring system, respectively.

NOESY Cross Peaks between the Hydrocarbon and DNA Protons. The intercalation of the trans(−)-DE2-(10*R*)−dA adduct was established by a total of 22 NOE cross peaks between the protons on the hydrocarbon ring system and adjacent DNA sugar protons. Approximately half (10) of these cross peaks were between T17 (the T on the unmodified strand base-paired to dA*6) and protons H1, H2, and H3 on one end of the hydrocarbon (Figure 8). Another three cross peaks were to protons H4, H5, and H6 along the outside edge (side nearest the major groove) of the hydrocarbon and the methyl group (Me) of T17 (Figure 8). A cross peak was also observed between dA*6 H2 and the inside edge (side nearest the minor groove) hydrocarbon proton H12. The remaining cross peaks were between the aliphatic protons H10 and H9 of the hydrocarbon and dC5 sugar and base protons of the modified strand. All of these cross peaks can only be satisfied if the hydrocarbon is intercalated from the

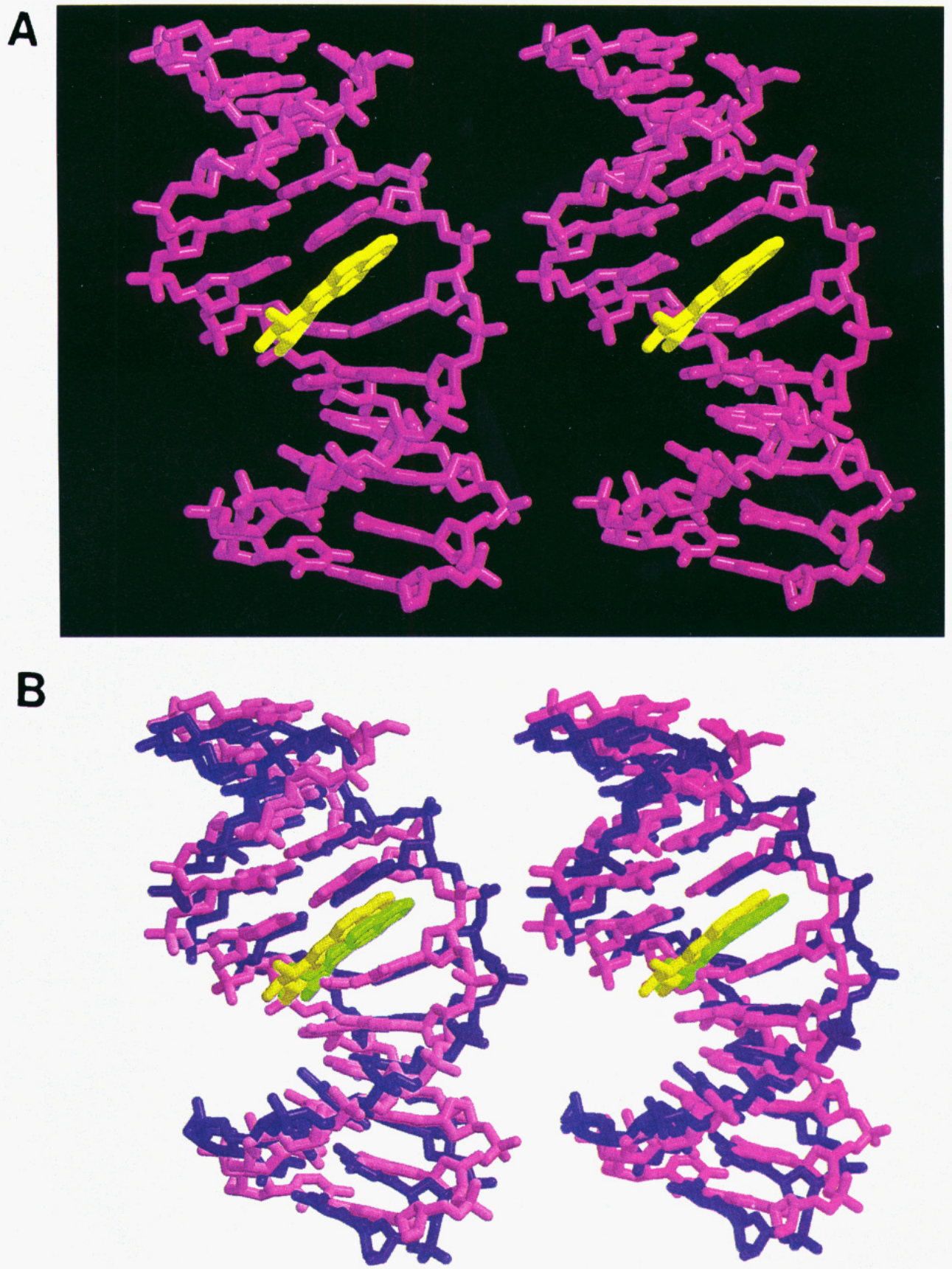

FIGURE 11: (A) Stereviews of the refined structure of the undecanucleotide duplex containing a trans (−)-DE1(10*R*)−dA adduct. Refinement started from a B-DNA model. The 5′ end of the modified strand is at the top with the view into the major groove. (B) Modified undecamer duplex refined from model-built B-DNA (magenta) overlaid with the same duplex refined from model-built A-DNA (blue). The 5′ end of the modified strand is at the top with the view into the major groove. The tetrahydrobenzo[*a*]pyrenyl ring is shown in yellow or green.

major groove between the dC5-dG18 and dA*6-T17 base pairs.

Chemical Shifts. Several unusual chemical shifts were observed for base protons that can be accounted for by the

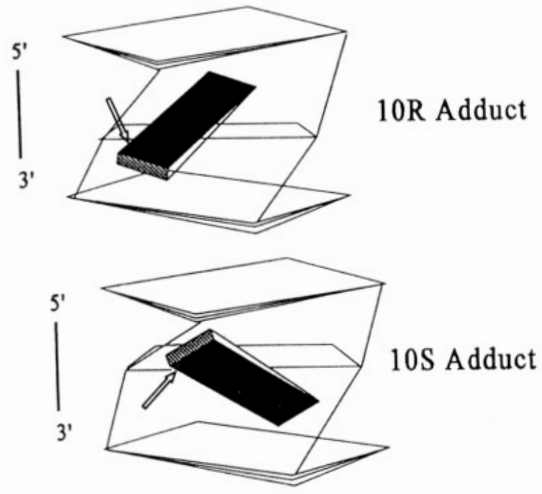

FIGURE 12: (Top) Schematic showing the hydrocarbon (black wedge) with *R* chirality at C10 [trans (−)-DE1(10*R*)−dA adduct)] is intercalated on the 5′ side of the modified adenine. The modified adenine is flanked by the neighboring bases. The view is into the major groove with the aliphatic portion of the hydrocarbon represented by the thick end of the wedge. (Bottom) Schematic showing the hydrocarbon with *S* chirality at C10 [trans (+)-DE1-(10*S*)−dA adduct)] intercalated on the 3′ side of the modified adenine. The point of attachment between the hydrocarbon and the adenine base is indicated by the arrow in each schematic structure.

intercalated orientation of the hydrocarbon. The dramatic upfield chemical shift of T17 Me protons mirrors the upfield shift of T17 H6. The shifts of T17 Me (−0.20 ppm) and T17 H6 (5.78 ppm) were due to direct stacking under the hydrocarbon (Figure 8). The H1′ proton of dG18 was not directly stacked over the aromatic ring (Figure 9); however, from its location it was possible to predict a 0.5 ppm upfield chemical shift (Jardetzky & Roberts, 1981) which was observed. The nonexchangeable protons of the hydrocarbon show a very similar chemical shift pattern to the intercalated structure of the trans (−)-DE2(10*R*)−dA adduct (Schurter et al., 1995) and the trans (+)-DE2(10*S*)−dA adduct (Yeh et al., submitted for publication) (Figure 10). This chemical shift pattern was distinct from that shown in the minor-groove structures of the trans (+)-DE2(10*S*)−dA adduct and trans (−)-DE2(10*R*)−dG adduct (Cosman et al., 1992; De los Santos et al., 1992).

Structural Refinement of the Benzo[a]pyrene−DNA Adduct. Two different starting model structures were considered: the plane of the pyrene moiety in the major groove perpendicular to the helical axis of both canonical A- and B-DNA. The NOESY spectra provided unambiguous evidence that dA*6 base was anti and the water/NOESY showed that it was base-paired to T17. The observed NOEs eliminated the possibilities that the hydrocarbon was in the minor groove or parallel to the helical axis.

The progress of the iterative MORASS/MD structural refinement for the hydrocarbon intercalated from the major groove starting with a B-DNA duplex backbone is shown in Table 4. All of the volumes merged by the third iteration, and the final total constraint energy penalty was 95 kcal/mol. As expected, no major changes during the iterative cycles were observed in the breakdown of the potential energies (E_{pot}) shown in Table 4 as well. There were 366 NOE distance constants incorporated into the refinement with 22 of them between the nonexchangeable hydrocarbon protons and DNA duplex sugar protons. The final RMS deviation between the theoretical and experimental volumes was 60% (corresponding to ~10% RMS deviation in the distances). The $Q(^1/_6)$ value decreased to 0.070, which corresponds to 7% RMS deviation in the $^1/_6$ power of the volumes.

The final refined structure (Figure 11A) shows the hydrocarbon intercalated from the major groove, between the dC5-dG18 and dA*-T17 base pairs. The modified deoxyadenosine dA*6 was in the anti conformation forming a normal Watson−Crick base pair to the opposite T. The hydrocarbon causes a slight counterclockwise displacement of the dC 5-dG18 base pair (as viewed from the top).

The iterative refinement from the model-built A-DNA duplex showed conversion of the A-DNA backbone to B-DNA by the third iteration. Overlaying the final structure refined from the A-DNA model with the final structure refined from B-DNA shows very good agreement (Figure 11B) with an RMS difference of 1.89 Å. The greatest deviation is toward the ends of the duplex with the site of the modification showing the least deviation.

DISCUSSION

The NOE refined structure of the adducted undecamer duplex $d(C_1G_2G_3T_4C_5A^*_6C_7G_8A_9G_{10}G_{11})$·$d(C_{12}C_{13}T_{14}C_{15}G_{16}T_{17}G_{18}A_{19}C_{20}C_{21}G_{22})$ was determined to have the hydrocarbon intercalated from the major groove between the dC5-dG18 and dA*6-T17 base pairs. The modified deoxyadenosine (dA*6) was in the anti conformation and retained Watson−Crick base pairing to T17 in the complementary strand.

In the present DE1 adduct, the tetrahydrobenzo ring assumes a boatlike conformation with the hydroxyl groups at C7 and C8 pseudoequatorial. This is confirmed by strong NOE cross peaks between the 1,3 diaxial protons, H10-H8 and H9-H7, with an interproton distance of 3 Å as opposed to 5 Å for the half-chair conformation. The boatlike conformation is in contrast to the half-chair conformation observed for the trans (−)-DE2(10*R*)−dA adduct in a nonanucleotide (Schurter et al., 1995). Monomeric nucleoside adducts of DE1 derived from BaP (Sayer et al., 1991) and other hydrocarbons [reviewed in Jerina et al. (1991)], as their fully acetylated derivatives in acetone, also generally prefer a half-chair conformation with pseudoaxial oxygen substituents at the positions corresponding to C7 and C8 of tetrahydro BaP, as indicated by coupling constants of 4.7−6.1 Hz for the corresponding pseudoequatorial protons.

The hydrocarbon intercalated from the major groove without significant disruption of either the anti glycosidic torsion angle of the modified dA residue or the base pairing between this residue and its complementary T. The pyrene moiety does not extend all the way through the DNA structure to the minor groove but instead has one edge (protons H3, H4, H5, and H6 of the hydrocarbon) partially exposed in the major groove. The present structure and an undecanucleotide duplex containing a trans DE2(10*R*)−dA adduct derived from benzo[*c*]phenanthrene with a complementary T (Cosman et al., 1993) both have the tetrahydrobenzo ring and the adjacent aromatic ring of the hydrocarbons similarly oriented relative to the DNA structure. In contrast, the hydrocarbon in the trans (−)-DE2(10*R*)−dA adduct with a dG mismatch (Schurter et al., 1995) exhibits a somewhat different intercalation geometry, with the hydrocarbon rotated around the N^6−C10 bond such that H5 and H6 are inside, and the opposite edge of the pyrene (H12,

Table 5: Melting Temperatures for Duplexes of the Unmodified Decamer, d(CGGTCA*CGAGG)·d(CCTCGTGACCG), Containing dA Adducts Derived from the Four Isomeric BaP Diol Epoxides with a T opposite the Modified dA[a]

adduct	T_m (°C)
DE2(10*S*)−dA	35
DE2(10*R*)−dA	43
DE1(10*S*)−dA	38
DE1(10*R*)−dA	47

[a] Melting curves were determined in 20 mM sodium phosphate buffer, pH 7, containing sufficient NaCl to give a total ionic strength of 100 mM. Concentration of the duplexes was 5 μM (10 μM total concentration of both strands).

H1, and H2) is pushed through the helix and extends into the minor groove.

The H3, H4, and H5 protons in the present structure have chemical shifts at lower field than in the trans (−)-DE2-(10*R*)−dA adduct with a dG mismatch since they extend into the major groove and are less shielded by the bases. This orientation of the hydrocarbon permits Watson−Crick base pairing to be maintained between the modified dA and its complementary T, as well as between the base pairs above and below the adduct intercalation site. In the dG mismatch (Schurter et al., 1995), base pairing to the modified dA with the anti conformation is not possible. Thus, the mispaired guanine is rotated out into the major groove and the hydrocarbon inserts into the pocket formed.

The modified oligonucleotide described in this study containing a trans (−)-DE1(10*R*)−dA adduct and that described previously containing a trans (−)-DE(10*R*)−dA adduct have the same absolute configuration at the point of attachment of the hydrocarbon to N^6 of adenine. Although an undecanucleotide was chosen for the present study in order to increase the stability (T_m) of the duplex, the local sequence context of the modified base is the same in both oligomers. Thus, comparisons between the two structures are not complicated by possible sequence-dependent differences. In both structures, the hydrocarbon is intercalated from the major groove and is located toward the 5′ end of the modified strand. Preliminary data (Yeh et al., submitted for publication) on the corresponding BaP trans (+)-DE2(10*S*)−dA adduct with the opposite configuration indicate that in this adduct the hydrocarbon is intercalated on the opposite side of the modified base and toward the 3′ end of the modified strand. The steric requirements for intercalation suggest that for all intercalated dA adducts of BaP, the pyrene rings must be in the same orientation relative to the DNA base pairs. The bottom face of the hydrocarbon when oriented as shown in Figure 1 will be toward the 3′ end of the modified strand, regardless of the stereochemistry of the hydroxyl groups or the absolute configuration at the point of attachment to the amino group of dA. Thus, when the hydrocarbon is intercalated from the major groove, carbons 11 and 12 will be nearest the minor groove and carbons 5 and 6 nearest the major groove regardless of whether intercalation is at the 3′ or 5′ side of the modified adenine. This orientation requires that adducts with 10*R* absolute configuration at C10 have the aromatic rings intercalated to the 5′ side of the modified adenine base and adducts with the opposite 10*S* absolute configuration have the aromatic rings to the 3′ side of the modified adenine. Similarly, an oligonucleotide with a different sequence containing a trans DE2(10*R*)−dA adduct derived from benzo[*c*]phenanthrene (BcPh) has the hydrocarbon intercalated on the 5′ side of the modified base (Cosman et al., 1993), whereas the oligonucleotide containing a BcPh adduct with the opposite configuration [DE2(10*S*)−dA adduct] has the hydrocarbon intercalated toward the 3′ side of the modified adenine (Cosman et al., 1995). An analogous but opposite effect of absolute configuration at C10 is observed for the trans 10*R* and trans 10*S* adducts derived from addition of the N^2-amino group of dG to the enantiomers of DE2, which lie in the minor groove oriented toward the 3′ and 5′ ends of the adducted strand, respectively (Cosman et al., 1992; De los Santos et al., 1992).

The hydrocarbon is tilted relative to the helix axis so that when the aromatic portion is intercalated to the 5′ side of the modified adenine (10*R* adduct) the aliphatic portion is out in the major groove and oriented toward the 3′ side of the modified adenine (Figure 12, top). This places the aliphatic end away from the DNA base pair on the 5′ side of the modified adenine. The base pair to the 3′ side of the modified adenine is rotated (due to the right-hand helical twist) away from the aliphatic portion of the hydrocarbon. The result is a minimum of steric interactions between the aliphatic portion of the hydrocarbon and the base pair to the 3′ side of the modified adenine. Similarly, when the aromatic portion of the hydrocarbon is intercalated to the 3′ side of the modified adenine (10*S* adduct), the aliphatic portion also extends out into the major groove and will be tilted toward the 5′ side of the modified adenine (Figure 12, bottom). Due to the right-handed helical twist, the aliphatic end of the hydrocarbon in this orientation will experience unfavorable steric interactions with the base pair 5′ to the modified adenine. This interaction may account for the decreased thermal stability (T_m = 16 °C) that is observed (Schurter et al., 1995) for a nonamer duplex containing a trans (+)-DE2-(10*S*)−dA adduct with a complementary T relative to that of the corresponding duplex containing a trans (−)-DE2-(10*R*)−dA adduct with a complementary T (T_m = 28 °C). Although the T_m of the nonamer duplex with a T opposite the (10*S*) dA adduct was too low to permit NMR study, an undecamer duplex with the same sequence as the oligonucleotide in this study and containing a trans DE2(10*S*)−dA adduct has a T_m of 35 °C (9 °C lower than the adduct of this study), and thus was a reasonable candidate for NMR. However, preliminary NMR data for this oligomer suggest that at least three conformational species are present, in roughly equal proportions. Examination of T_m data for the undecamers containing dA adducts derived from the four isomeric BaP diol epoxides (Table 5) shows a pattern of lower thermal stability for the 10*S* as contrasted with the 10*R* adducts when the complementary base is a T.

REFERENCES

Bax, A., & Davis, D. G. (1985) *J. Magn. Reson. 65*, 355−360.

Boelens, R., Koning, T., & Kaptein, R. (1988) *J. Mol. Struct. 173*, 299−311.

Boelens, R., Koning, T., van der Marel, G., van Boom, J., & Kaptein, R. (1989) *J. Magn. Reson. 82*, 290−308.

Bonvin, A. M. J. J., Rullmann, J. A. C., Lamerichs, R. M. J. N., Boelens, R., & Kaptein, R. (1993) *Proteins: Struct., Funct., Genet. 15*, 385−400.

Chang, R. L., Wood, A. W., Conney, A., II., Yagi, H., Sayer, J. M., Thakker, D. R., Jerina, D. M., & Levin, W. (1987) *Proc. Natl. Acad. Sci. U.S.A. 84*, 8633−8636.

Cosman, M., De los Santos, C., Fiala, R., Hingerty, B. E., Sigh, S. B., Ibanez, V., Margulis, L., Live, D., Geacintov, N. E., Broyde, S., & Patel, D. J. (1992) *Proc. Natl. Acad. Sci. U.S.A. 89*, 1914−1918.

Cosman, M., Fiala, R., Hingerty, B. E., Laryea, A., Lee, H., Harvey, R. G., Amin, S., Geacintov, N. E., Broyde, S., & Patel, D. J. (1993) *Biochemistry 32*, 12488−12497.

Cosman, M., Laryea, A., Fiala, R., Hingerty, B. E., Amin, S., Geacintov, N. E., Broyde, S., & Patel, D. J. (1995) *Biochemistry 34*, 1295−1307.

De los Santos, C., Cosman, M., Hingerty, B. E., Ibanez, V., Margulis, L. A., Geacintov, N. E., Broyde, S., & Patel, D. J. (1992) *Biochemistry 31*, 5245−5252.

Ferrin, T. E., Huang, C. C., Jarvis, L. C., & Langridge, R. (1988) *J. Mol. Graphics 6*, 13−27.

Gorenstein, D. G., Meadows, R., Metz, J. T., Nikonowicz, E., & Post, C. B. (1990) in *Advances in Biophysical Chemistry* (Bush, C. A., Ed.) Vol. 1, pp 47−124, JAI Press, Greenwich, CT.

Gorenstein, D. G., Luxon, B. A., Post, C. B., & Meadows, R. (1993) MORASS2.0 Program, Purdue University, W. Lafayette, IN.

Hingerty, B. E., & Broyde, S. (1985) *Biopolymers 24*, 2279−2299.

James, T. L., Thomas, P. D., & Basos, V. J. (1991) *Proc. Natl. Acad. Sci. U.S.A. 88*, 1237−1241.

Jardetzky, O., & Roberts, J. G. (1981) *NMR in Molecular Biology*, Academic Press, New York.

Jerina, D. M., & Daly, J. W. (1976) in *Drug Metabolism—from Microbe to Man* (Parke, D. V., & Smith, R. L., Eds.) pp 13−32, Taylor and Francis Ltd., London.

Jerina, D. M., Lehr, R. E., Yagi, II, Hernandez, O., Dansette, P. G., Wood, A. W., Chang, R. L., Levin, W., & Conney, A. H. (1976) in *In Vitro Metabolic Activation in Mutagenesis Testing* (de Serres, F. J., Fouts, J. R., Bend, J. R., & Philpot, R. M., Eds.) pp 159−177, Elsevier/North-Holland Biomedical Press, Amsterdam.

Jerina, D. M., Yagi, H., Thakker, D. R., Lehr, R. E., Wood, A. W., Levin, W., & Conney, A. H. (1980) in *Microsomes, Drug Oxidations, and Chemical Carcinogenesis* (Coon, M. J., Conney, A. H., Eastbrook, R. W., Gelboin, H. V., Gillette, J. R., & O'Brian, P., Eds.) pp 1041−1051, Academic Press, Inc., New York.

Jerina, D. M., Yagi, H., Thakker, D. R., Sayer, J. M., van Bladeren, P. J., Lehr, R. E., Whalen, D. L., Levin, W., Chang, R. L., Wood, A., & Conney, A. H. (1984) in *Foreign Compound Metabolism* (Caldwell, J., & Paulson, G. D., Eds.) pp 257−266, Taylor and Francis Ltd., London.

Jerina, D. M., Chadha, A., Cheh, A. M., Schurdak, M. E., Wood, A. W., & Sayer, J. M. (1991) in *Biological Reactive Intermediates IV. Molecular and Cellular Effects and Their Impact on Human Health* (Wittmer, C. M., Snyder, R., Jollow, D. J., Kalf, G. E., Kocsis, J. J., & Sipes, I. G., Eds.) pp 533−553, Plenum Press, New York.

Keepers, J. W., & James, T. L. (1984) *J. Magn. Reson. 57*, 404−426.

Lakshman, M. K., Sayer, J. M., Yagi, H., & Jerina, D. M. (1992) *J. Org. Chem. 57*, 4584−4590.

Nikonowicz, E., Meadows, R., Post, C., Jones, C., & Gorenstein, D. G. (1989) *Bull. Magn. Reson. 11*, 226−229.

Nikonowicz, E., Meadows, R., & Gorenstein, D. G. (1990) *Biochemistry 29*, 4193−4204.

Ottings, G., Liepinsh, E., Farmer, B. T., II, & Wüthrich, K. (1991) *J. Biomol. NMR 1*, 209−215.

Patel, D. J., Broyde, S., Geacintov, N. E., Harvey, R., Luna, E., Ibanez, V., Hingerty, B. E., Fiala, R., De los Santos, C., & Cosman, M. (1993) *Biochemistry 32*, 4145−4155.

Sayer, J. M., Chadha, A., Agarwal, S. K., Yeh, H. J. C., Yagi, H., & Jerina, D. M. (1991) *J. Org. Chem. 56*, 20−29.

Schurter, E. J., Yeh, H. J. C., Sayer, J. M., Lakshman, M. K., Yagi, H., Jerina, D. M., & Gorenstein, D. G. (1995) *Biochemistry 34*, 1364−1375.

Thakker, D. R., Yagi, H., Akagi, H., Koreeda, M., Lu, A. Y. H., Levin, W., Wood, A. W., Conney, A. H., & Jerina, D. M. (1977) *Chem. Biol. Interact. 16*, 281−300.

Thakker, D. R., Yagi, H., Levin, W., Wood, A. W., Conney, A. H., & Jerina, D. M. (1985) in *Bioactivation of Foreign Compounds* (Anders, M. W., Ed.) pp 177−242, Academic Press, New York.

Thakker, D. R., Levin, W., Wood, A. W., Conney, A. H., Yagi, H., & Jerina, D. M. (1988) in *Drug Stereochemistry—Analytical Methods and Pharmacology* (Wainer, I. W., & Drayer, D. E., Eds.) pp 271−296, Marcel Dekker, Inc., New York.

Wei, S.-J. C., Chang, R. L., Wong, C.-Q., Bhachech, N., Cui, X. X., Hennig, E., Yagi, H., Sayer, J. M., Jerina, D. M., Preston, B. D., & Conney, A. H. (1991) *Proc. Natl. Acad. Sci. U.S.A. 88*, 11227−11230.

Wei, S.-J. C., Chang, R. L., Bhachech, N., Cui, X. X., Merkler, K. A., Wong, C.-Q., Hennig, E., Yagi, H., Jerina, D. M., & Conney, A. H. (1993) *Cancer Res. 53*, 3294−3301.

Weiner, P. K., & Kollman, P. A. (1981) *J. Comput. Chem. 2*, 287−303.

Wüthrich, K. (1986) *NMR of Proteins and Nucleic Acids*, Wiley, New York.

BI942424+